ENHANCED MODEL ORDER ESTIMATION USING HIGHER-ORDER ARRAYS

João Paulo C. L. da Costa, Martin Haardt, Florian Römer, and Giovanni Del Galdo

Ilmenau University of Technology, Communications Research Laboratory
P.O. Box 10 05 65, D-98684 Ilmenau, Germany, http://www.tu-ilmenau.de/crl
{joaopaulo.dacosta, martin.haardt, florian.roemer}@tu-ilmenau.de

***Abstract* — Frequently, R-dimensional subspace-based methods are used to estimate the parameters in multi-dimensional harmonic retrieval problems in a variety of signal processing applications. Since the measured data is multi-dimensional, traditional approaches require stacking the dimensions into one highly structured matrix. Recently, we have shown how an HOSVD based low-rank approximation of the measurement tensor leads to an improved signal subspace estimate, which can be exploited in any multi-dimensional subspace-based parameter estimation scheme. To achieve this goal, it is required to estimate the model order of the multi-dimensional data.**

In this paper, we show how the HOSVD of the measurement tensor also enables us to improve the model order estimation step. This is due to the fact that only one set of eigenvalues is available in the matrix case. Applying the HOSVD, we obtain $R+1$ sets of n-mode singular values of the measurement tensor that are used jointly to improve the accuracy of the model order selection significantly.

1. INTRODUCTION

Multi-dimensional subspace-based estimation problems are encountered in a variety of signal processing applications including radar, sonar, communications, channel modeling, medical imaging, and the estimation of the parameters of the dominant multipath components from MIMO channel measurements. Since the measured data is multi-dimensional, traditional approaches require stacking the dimensions into one highly structured matrix. In [9], we have shown how a higher-order SVD (HOSVD) based low-rank approximation of the measurement tensor leads to an improved signal subspace estimate, which can be exploited in any multi-dimensional subspace-based estimation scheme. To achieve this goal, it is required to estimate the model order of the multi-dimensional data.

State-of-the-art model order estimation techniques include information theoretic criteria such as Akaike's information theoretic criterion (AIC) [1], [10] and the Minimum Description Length (MDL) criterion [2], [10]. These classical model order selection methods often fail when the number of available snapshots is small. To deal with these cases, the Exponential Fitting Test (EFT) has been developed in [4], [8]. For short data records in additive white Gaussian noise, the profile of the ordered noise eigenvalues approximately fits an exponential law. This fact is used to provide an algorithm that detects a mismatch between the observed eigenvalue profile and the theoretical noise-only eigenvalue profile. Thereby, we identify the noise eigenvalues and consequently the number of signal eigenvalues, i.e., the number of sources.

The remainder of this paper is organized as follows. After reviewing the tensor and matrix notation in Section 2, the data model of the R-dimensional harmonic retrieval is presented as an example for multi-dimensional subspace based estimation problems in Section 3. Then the modified Exponential Fitting Test (M EFT) is developed in Section 4, before its R-D extension is covered in Section 5. In particular, we show how the HOSVD of the measurement tensor also enables us to improve the model order estimation step. This is due to the fact that only one set of eigenvalues is available in the matrix case. Applying the HOSVD, we obtain $R+1$ sets of n-mode singular values of the measurement tensor that are combined to form *global eigenvalues*. Thereby, we improve the model order selection accuracy of the EFT significantly as compared to the matrix case. Inspired by the good performance of the R-D EFT, we also propose similar R-D extensions of other model order selection algorithms such as AIC or MDL. The simulation results in Section 6 confirm the improved performance of these R-D techniques.

2. TENSOR AND MATRIX NOTATION

In order to facilitate the distinction between scalars, matrices, and tensors, the following notation is used: Scalars are denoted as italic letters ($a, b, \ldots, A, B, \ldots, \alpha, \beta, \ldots$), column vectors as lower-case bold-face letters ($\boldsymbol{a}, \boldsymbol{b}, \ldots$), matrices as bold-face capitals ($\boldsymbol{A}, \boldsymbol{B}, \ldots$), and tensors are written as bold-face calligraphic letters ($\boldsymbol{\mathcal{A}}, \boldsymbol{\mathcal{B}}, \ldots$). Lower-order parts are consistently named: the (i, j)-element of the matrix $\boldsymbol{A}$, is denoted as $a_{i,j}$ and the (i, j, k)-element of a third order tensor $\boldsymbol{\mathcal{X}}$ as $x_{i,j,k}$. The n-mode vectors of a tensor are obtained by varying the n-th index within its range $(1, 2, \ldots, I_n)$ and keeping all the other indices fixed.

We use the superscripts ^{T}, ^{H}, $^{-1}$, $^+$ and * for transposition, Hermitian transposition, matrix inversion, the Moore-Penrose pseudo inverse of matrices, and complex conjugation, respectively. Moreover the Khatri-Rao product (columnwise Kronecker product) is denoted by $\boldsymbol{A} \diamond \boldsymbol{B}$.

The tensor operations we use are consistent with [3]: **The n-mode product** of a tensor $\boldsymbol{\mathcal{A}} \in \mathbb{C}^{I_1 \times I_2 \times \ldots \times I_N}$ and a matrix $\boldsymbol{U} \in \mathbb{C}^{J_n \times I_n}$ along the n-th mode is denoted as $\boldsymbol{\mathcal{A}} \times_n \boldsymbol{U} \in \mathbb{C}^{I_1 \times I_2 \ldots \times J_n \ldots \times I_N}$. It is obtained by multiplying all n-mode vectors of $\boldsymbol{\mathcal{A}}$ from the left-hand side by the matrix $\boldsymbol{U}$.

João Paulo C. L. da Costa is a scholarship holder of the National Counsel of Technological and Scientific Development (Conselho Nacional de Desenvolvimento Científico e Tecnológico, CNPq) of the Brazilian Government and also a First Lieutenant of the Brazilian Army (Exército Brasileiro).

The higher order SVD (HOSVD) of a tensor $\boldsymbol{\mathcal{A}} \in \mathbb{C}^{I_1 \times I_2 \times \ldots \times I_N}$ is given by

$$\boldsymbol{\mathcal{A}} = \boldsymbol{\mathcal{S}} \times_1 \boldsymbol{U}_1 \times_2 \boldsymbol{U}_2 \ldots \times_N \boldsymbol{U}_N, \tag{1}$$

where $\boldsymbol{\mathcal{S}} \in \mathbb{C}^{I_1 \times I_2 \times \ldots \times I_N}$ is the core-tensor which satisfies the all-orthogonality conditions [3] and $\boldsymbol{U}_n \in \mathbb{C}^{I_n \times I_n}$, $n = 1, 2, \ldots, N$ are the unitary matrices of n-mode singular vectors.

Finally, the n-mode unfolding of a tensor $\boldsymbol{\mathcal{A}}$ is symbolized by $\boldsymbol{\mathcal{A}}_{(n)} \in \mathbb{C}^{I_n \times (I_1 I_2 \ldots I_{n-1} I_{n+1} \ldots I_N)}$, i.e., it represents the matrix of n-mode vectors of the tensor $\boldsymbol{\mathcal{A}}$. The order of the columns is chosen in accordance with [3].

3. DATA MODEL

As an example for the model order estimation schemes discussed in this paper, consider the R-dimensional harmonic retrieval problem under the assumption that the data is sampled on an R-dimensional lattice. A typical application is the parameter estimation step which follows channel sounding [6]. From the multi-dimensional channel measurements it is possible to retrieve parameters such as directions of arrival (DOAs), directions of departure (DODs), Doppler shifts and time delays of arrival (TDOAs) of dominant specular components.

In general, the observations may be modeled as a superposition of d damped exponentials sampled on an R-dimensional grid of size $M_1 \times M_2 \times \ldots \times M_R$ at N subsequent time instants. The measurement samples are given by

$$\begin{aligned} x_{m_1,m_2,\ldots,m_R,n} &= \sum_{i=1}^{d} s_i(n) \prod_{r=1}^{R} e^{(m_r-1)\cdot\left(\zeta_i^{(r)} + j\cdot\mu_i^{(r)}\right)} \\ &\quad + n_{m_1,m_2,\ldots,m_R,n}, \end{aligned} \tag{2}$$

where $m_r = 1, 2, \ldots, M_r$ for $r = 1, 2, \ldots, R$, $n = 1, 2, \ldots, N$, $s_i(n)$ denotes the complex amplitude of the i-th exponential at time instant n, $\mu_i^{(r)}$ symbolizes the spatial frequency of the i-th exponential in the r-th mode, $\zeta_i^{(r)} \leq 0$ represents the corresponding damping factor, and $n_{m_1,m_2,\ldots,m_R,n}$ models the additive noise component inherent in the measurement process. In the context of array signal processing, each of the exponentials represents one planar wavefront and the complex amplitudes $s_i(n)$ are the symbols. It is our goal to estimate the number of impinging signals d.

In the classical matrix approach, (2) is transformed into a matrix-vector equation by defining an array steering matrix [5]

$$\begin{aligned} \boldsymbol{A} &= \boldsymbol{A}^{(1)} \diamond \boldsymbol{A}^{(2)} \ldots \diamond \boldsymbol{A}^{(R)} \in \mathbb{C}^{M \times d} \\ \boldsymbol{A}^{(r)} &= \left[\boldsymbol{a}^{(r)}\left(\mu_1^{(r)}\right),\ \boldsymbol{a}^{(r)}\left(\mu_2^{(r)}\right),\ \ldots,\ \boldsymbol{a}^{(r)}\left(\mu_d^{(r)}\right)\right], \end{aligned} \tag{3}$$

where $M = \prod_{r=1}^{R} M_r$ and the vector $\boldsymbol{a}^{(r)}\left(\mu_i^{(r)}\right) \in \mathbb{C}^{M_r \times 1}$ denotes the array response in the r-th dimension for the i-th source. Here, all the spatial dimensions are stacked into column vectors. This stacking operation allows us to write the measurement equation in matrix form

$$\boldsymbol{X} = \boldsymbol{A} \cdot \boldsymbol{S} + \boldsymbol{N}, \tag{4}$$

where $\boldsymbol{X} \in \mathbb{C}^{M \times N}$ now contains the measurements stacked in a similar fashion as in $\boldsymbol{A}$, the matrix $\boldsymbol{S} \in \mathbb{C}^{d \times N}$ contains the symbols $s_i(n)$ and the noise samples are collected in the matrix $\boldsymbol{N} \in \mathbb{C}^{M \times N}$. It is obvious that the stacking operation does not capture the structure inherent in the lattice that is used to sample the data.

We therefore replace the measurement matrix $\boldsymbol{X}$ by a measurement tensor $\boldsymbol{\mathcal{X}} \in \mathbb{C}^{M_1 \times M_2 \times \ldots \times M_R \times N}$. Its elements are given by (2). Similarly to (4), $\boldsymbol{\mathcal{X}}$ can be modeled as

$$\boldsymbol{\mathcal{X}} = \boldsymbol{\mathcal{A}} \times_{R+1} \boldsymbol{S}^T + \boldsymbol{\mathcal{N}}. \tag{5}$$

Here the matrix $\boldsymbol{S}$ is the same as in (4), the tensor $\boldsymbol{\mathcal{N}}$ contains the noise samples as defined in (2), and the tensor $\boldsymbol{\mathcal{A}} \in \mathbb{C}^{M_1 \times M_2 \times \ldots \times M_R \times d}$ is termed the array steering tensor. It can be computed from the array response vectors $\boldsymbol{a}^{(r)}(\mu_i^{(r)})$ through the outer product operator. Its i-th slice in the $(R+1)$-th mode is given by

$$\boldsymbol{\mathcal{A}}_{i_{R+1}=i} = \boldsymbol{a}^{(1)}\left(\mu_i^{(1)}\right) \circ \boldsymbol{a}^{(2)}\left(\mu_i^{(2)}\right) \circ \ldots \circ \boldsymbol{a}^{(R)}\left(\mu_i^{(R)}\right), \tag{6}$$

$i = 1, 2, \ldots, d$. Consequently, in the absence of noise, (5) may be rewritten as

$$\boldsymbol{\mathcal{X}} = \sum_{i=1}^{d} \boldsymbol{a}^{(1)}\left(\mu_i^{(1)}\right) \circ \boldsymbol{a}^{(2)}\left(\mu_i^{(2)}\right) \circ \ldots \circ \boldsymbol{a}^{(R)}\left(\mu_i^{(R)}\right) \circ \boldsymbol{s}_i^T, \tag{7}$$

where $\boldsymbol{s}_i^T$ is the i-th row of $\boldsymbol{S}$. An important consequence we can draw from (7) is that, in the absence of noise, the tensor $\boldsymbol{\mathcal{X}}$ has rank d.[1] Therefore, all the n-ranks of $\boldsymbol{\mathcal{X}}$ are at most d. Note that the matrix and tensor data model are connected through the relations $\boldsymbol{A}^T = [\boldsymbol{\mathcal{A}}]_{(R+1)}$ and $\boldsymbol{X}^T = [\boldsymbol{\mathcal{X}}]_{(R+1)}$.

To simplify the notation, let us consider the temporal dimension as dimension $(R+1)$, so that $M_{R+1} = N$. Moreover, let $M = \prod_{r=1}^{R} M_r$. For the r-mode unfolding we define the sample covariance matrix as

$$\hat{\boldsymbol{R}}_{xx}^{(r)} = \frac{M_r}{M \cdot N} \boldsymbol{\mathcal{X}}_{(r)} \cdot \boldsymbol{\mathcal{X}}_{(r)}^H \in \mathbb{C}^{M_r \times M_r}. \tag{8}$$

The eigenvalues of these sample covariance matrices play a major role in the model order estimation step. Let us denote the i-th eigenvalue of the sample covariance matrix of the r-mode unfolding as $\lambda_i^{(r)}$. Notice that $\hat{\boldsymbol{R}}_{xx}^{(r)}$ possesses M_r eigenvalues, which we order in such a way that $\lambda_1^{(r)} \geq \lambda_2^{(r)} \geq \ldots \lambda_{M_r}^{(r)}$. The eigenvalues may be computed from the HOSVD of the measurement tensor

$$\boldsymbol{\mathcal{X}} = \boldsymbol{\mathcal{S}} \times_1 \boldsymbol{U}_1 \times_2 \boldsymbol{U}_2 \ldots \times_{R+1} \boldsymbol{U}_{R+1} \tag{9}$$

as

$$\operatorname{diag}\left(\lambda_1^{(r)}, \lambda_2^{(r)}, \ldots, \lambda_{M_r}^{(r)}\right) = \frac{M_r}{M \cdot N} \boldsymbol{\mathcal{S}}_{(r)} \cdot \boldsymbol{\mathcal{S}}_{(r)}^H. \tag{10}$$

Note that the eigenvalues $\lambda_i^{(r)}$ are related to the r-mode singular values $\sigma_i^{(r)}$ of $\boldsymbol{\mathcal{X}}$ through $\lambda_i^{(r)} = \frac{M_r}{M \cdot N}\left(\sigma_i^{(r)}\right)^2$.

Classical approaches to model order selection require the computation of the sample covariance matrix $\hat{\boldsymbol{R}}_{xx}$ and of its eigenvalues, obtained from the measurement matrix $\boldsymbol{X}$ via

$$\hat{\boldsymbol{R}}_{xx} = \frac{1}{N} \boldsymbol{X} \cdot \boldsymbol{X}^H \in \mathbb{C}^{M \times M}. \tag{11}$$

[1] The rank cannot be larger than d, but it might be smaller. This occurs only in degenerate cases which are not relevant for our discussion, e.g., two coherent sources at exactly the same position.

Notice that the non-zero eigenvalues are identical to those computed from the $(R+1)$-mode unfolding using (10).

A frequently encountered special case is the presence of *undamped* exponentials, i.e., $\zeta_i^{(r)} = 0 \ \forall i = 1, 2, \ldots, d, \forall r = 1, 2, \ldots, R$. In this case we can enhance the performance further by incorporating forward-backward averaging as a preprocessing step [11]. Thereby, we virtually double the number of available snapshots without sacrificing array aperture. In the matrix case, forward-backward averaging [11] may be incorporated by replacing the measurement matrix $\boldsymbol{X} \in \mathbb{C}^{M \times N}$ by a modified matrix $\boldsymbol{Z} \in \mathbb{C}^{M \times 2N}$ given by [5]

$$\boldsymbol{Z} = [\boldsymbol{X} \quad \boldsymbol{\Pi}_M \boldsymbol{X}^* \boldsymbol{\Pi}_N], \tag{12}$$

where $\boldsymbol{\Pi}_n$ represents the $n \times n$ exchange matrix having ones on its anti-diagonal and zeros elsewhere. In [9] it was demonstrated that in the tensor case, forward-backward averaging can be expressed in the following form

$$\boldsymbol{\mathcal{Z}} = [\boldsymbol{\mathcal{X}} \sqcup_{R+1} \boldsymbol{\mathcal{X}}^* \times_1 \boldsymbol{\Pi}_{M_1} \ldots \times_R \boldsymbol{\Pi}_{M_R} \times_{R+1} \boldsymbol{\Pi}_N], \tag{13}$$

where $[\boldsymbol{\mathcal{A}} \sqcup_n \boldsymbol{\mathcal{B}}]$ represents the concatenation of two tensors $\boldsymbol{\mathcal{A}}$ and $\boldsymbol{\mathcal{B}}$ along the n-th mode.

In model order selection schemes, forward-backward averaging is incorporated by replacing the data matrix $\boldsymbol{X}$ in (11) by $\boldsymbol{Z}$ or the data tensor $\boldsymbol{\mathcal{X}}$ in (9) by $\boldsymbol{\mathcal{Z}}$. Moreover, we have to replace N by $2N$ in the subsequent formulas since the number of snapshots is virtually doubled.

To reduce the computational complexity, the forward-backward averaged data matrix $\boldsymbol{Z}$ can be replaced by a real-valued data matrix $\varphi\{\boldsymbol{Z}\} \in \mathbb{R}^{M \times 2N}$ which has the same singular values as $\boldsymbol{Z}$ [7]. This transformation can be extended to the tensor case where the forward-backward averaged data tensor $\boldsymbol{\mathcal{Z}}$ is replaced by a real-valued data tensor $\varphi\{\boldsymbol{\mathcal{Z}}\} \in \mathbb{R}^{M_1 \times \ldots \times M_R \times 2N}$ possessing the same r-mode singular values for all $r = 1, 2, \ldots, R+1$ (see [9] for details).

4. MODIFIED EXPONENTIAL FITTING TEST (M EFT)

Classical approaches to model order estimation, such as the Akaike Information Criterion (AIC) and Rissanen's Minimum Description Length (MDL), are based on the matrix representation shown in (4) and on the sample covariance matrix expressed in (11). In particular, their application to antenna array processing has been studied in [10].

These methods often fail when the number of independent temporal snapshots N is small. The Exponential Fitting Test (EFT) [8] can be effectively used in such cases. This technique is based on the observation that, in a noise-only case, the profile of the ordered eigenvalues can be well approximated by a decaying exponential.

Let λ_i be the i-th eigenvalue of the sample covariance matrix in (11). The exponential model may be expressed as

$$\mathrm{E}\{\lambda_i\} = \mathrm{E}\{\lambda_1\} \cdot q(\alpha, \beta)^{i-1}, \tag{14}$$

where $\mathrm{E}\{\cdot\}$ is the expectation operator and we assume that the eigenvalues are sorted so that λ_1 is the largest. The term $q(\alpha, \beta)$ is defined as

$$q(\alpha, \beta) = \tag{15}$$
$$\exp\left\{-\sqrt{\frac{30}{\alpha^2+2} - \sqrt{\frac{900}{(\alpha^2+2)^2} - \frac{720\alpha}{\beta(\alpha^4+\alpha^2-2)}}}\right\}$$

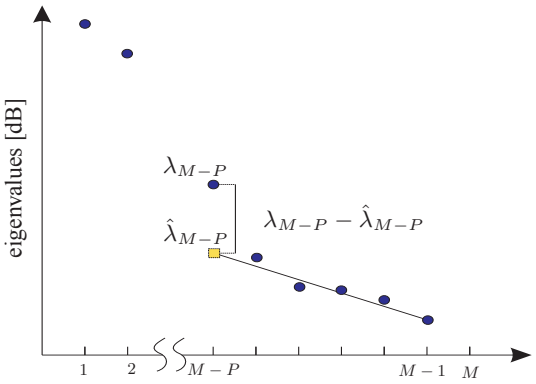

Fig. 1. Typical profile of the eigenvalues (EVs). The last $P-1$ EVs are used to estimate the $(M-P)$-th EV, denoted by a yellow square. The EFT method considers the gap between the real EV and the estimated one.

so that $0 < q(\alpha, \beta) < 1$. In reference [8] it was proposed to set $\alpha = M$ and $\beta = N$ assuming that $M \leq N$. As a *first modification*, we propose to set $\alpha = \min\{M, N\}$ and $\beta = \max\{M, N\}$ for any values of M and N.

Next, consider the case of d non-coherent sources corrupted by additive noise. Then, the $M-d$ noise eigenvalues still exhibit a decaying exponential profile. Let P denote the number of candidate noise eigenvalues. The basic idea behind the EFT method is to choose the highest P for which the candidate noise eigenvalues can be well fitted to the theoretical decaying exponential. Moreover, the method assumes that there is at least one noise eigenvalue, i.e., $d < M$. For each value of P in the range $1 \leq P \leq M-1$ we find the parameters of the decaying exponential which best fit the observations and we compute the prediction for the $(M-P)$-th eigenvalue, which we denote by $\hat{\lambda}_{M-P}$. The latter can be found as follows

$$\hat{\lambda}_{M-P} = (P+1)\,\frac{1 - q(P+1, N)}{1 - q(P+1, N)^{P+1}}\,\hat{\sigma}^2 \tag{16}$$

$$\hat{\sigma}^2 = \frac{1}{P}\sum_{i=0}^{P-1} \lambda_{M-i}. \tag{17}$$

Thereby, it is possible to obtain $M-1$ predicted eigenvalues, namely $\hat{\lambda}_{M-P}$ for $1 \leq P \leq M-1$. In (17) we propose a *second modification* of the original EFT by calculating $\hat{\sigma}^2$ as the average of the P smallest eigenvalues instead of the taking the average of the $P+1$ smallest eigenvalues as originally proposed in [4] and [8]. To decide whether the $(M-P)$-th eigenvalue λ_{M-P} fits to the exponential profile we measure its relative distance to the predicted eigenvalue $\hat{\lambda}_{M-P}$. By setting a threshold η_P we can formulate the following hypotheses:

$$\begin{aligned} H_{P+1}&: \ \lambda_{M-P} \text{ is a noise EV}, \ \frac{\lambda_{M-P} - \hat{\lambda}_{M-P}}{\hat{\lambda}_{M-P}} \leq \eta_P \\ \bar{H}_{P+1}&: \ \lambda_{M-P} \text{ is a signal EV}, \ \frac{\lambda_{M-P} - \hat{\lambda}_{M-P}}{\hat{\lambda}_{M-P}} > \eta_P. \end{aligned} \tag{18}$$

The largest P for which the test H_{P+1} fails, denoted by P_{opt}, determines the estimated model order $\hat{d} = M - P_{\mathrm{opt}}$. In the

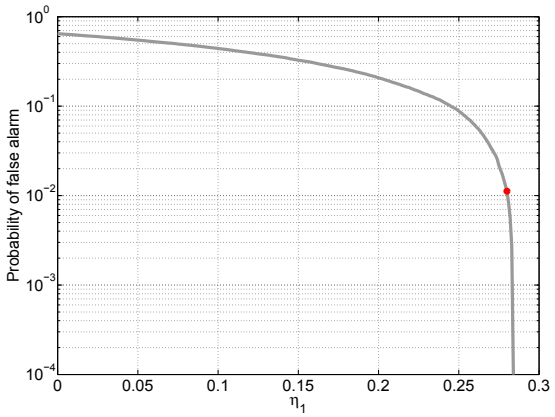

Fig. 2. Functional dependency between the probability of false alarm $P_{\text{fa}}(P)$ and the threshold η_P. The plot corresponds to $M = 5$, $N = 6$, and $P = 1$.

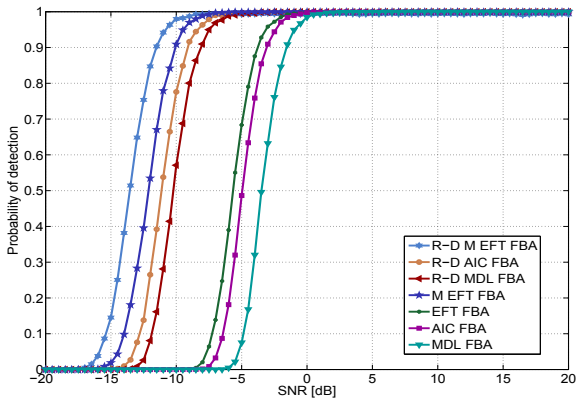

Fig. 3. Probability of detection vs. SNR for an array of size $M_1 = 5$, $M_2 = 7$, and $M_3 = 9$. The number of snapshots N is set to 10 and the number of sources $d = 3$.

example depicted in Figure 1, the exponential profile is fitted to the last $P-1$ eigenvalues. The $(M-P)$-th eigenvalue λ_{M-P} is then compared to the predicted eigenvalue $\hat{\lambda}_{M-P}$.

The thresholds η_P are obtained by Monte Carlo simulations carried out in the noise-only case. To this end, we define the *conditional probability of false alarm* as $P_{\text{fa}}(P) = \Pr(\bar{H}_{P+1}|H_2, H_3, \ldots, H_P)$. It expresses the probability of detecting a signal for the $(M-P-1)$-th eigenvalue conditioned on the fact that the smallest P eigenvalues are correctly identified as noise. By considering a large number of realizations it is possible to obtain the functional dependency of η_P on $P_{\text{fa}}(P)$. By setting $P_{\text{fa}}(P)$ to an appropriate value (such as 0.01), we can obtain a numerical value for η_P. Such a function is plotted in Figure 2.

5. R-D EXPONENTIAL FITTING TEST (R-D EFT)

To derive the proposed extension of the EFT algorithm, namely the R-D EFT, we start by looking at an $(R+1)$-dimensional noise-only case. For the r-th dimension, the eigenvalues of the sample covariance matrix $\hat{\boldsymbol{R}}_{xx}^{(r)}$ in equation (8), denoted by $\lambda_i^{(r)}$, will display the same exponential profile modeled in (14), namely

$$\mathrm{E}\left\{\lambda_i^{(r)}\right\} = \mathrm{E}\left\{\lambda_1^{(r)}\right\} \cdot q(\alpha_r, \beta_r)^{i-1}, \tag{19}$$

where $\alpha_r = \min\{M_r, N\}$ and $\beta_r = \max\{M_r, N\}$. Once more we assume that the eigenvalues are sorted so that $\lambda_1^{(r)}$ is the largest.

Let us now consider a case in which all modes have the same dimension, so that $M_1 = M_2 = \ldots = M_{R+1}$. We can define a new set of eigenvalues $\lambda_i^{(\mathrm{G})}$, which we refer to as the *global eigenvalues*, as

$$\lambda_i^{(\mathrm{G})} = \lambda_i^{(1)} \cdot \lambda_i^{(2)} \cdot \ldots \cdot \lambda_i^{(R+1)}. \tag{20}$$

Then, we can show that

$$\mathrm{E}\left\{\lambda_i^{(\mathrm{G})}\right\} = \mathrm{E}\left\{\lambda_1^{(\mathrm{G})}\right\} \cdot \left(q(\alpha_1, \beta_1) \cdot \ldots \cdot q(\alpha_{R+1}, \beta_{R+1})\right)^{i-1}.$$

This allows us to apply the modified EFT in the way summarized in the previous section. In particular, the hypotheses defined in equation (18) for the tensor case become

$$\begin{aligned} H_{P+1}:\ & \lambda_{M-P}^{(\mathrm{G})} \text{ is a noise EV}, & \frac{\lambda_{M-P}^{(\mathrm{G})} - \hat{\lambda}_{M-P}^{(\mathrm{G})}}{\hat{\lambda}_{M-P}^{(\mathrm{G})}} &\leq \eta_P^{(\mathrm{G})} \\ \bar{H}_{P+1}:\ & \lambda_{M-P}^{(\mathrm{G})} \text{ is a signal EV}, & \frac{\lambda_{M-P}^{(\mathrm{G})} - \hat{\lambda}_{M-P}^{(\mathrm{G})}}{\hat{\lambda}_{M-P}^{(\mathrm{G})}} &> \eta_P^{(\mathrm{G})}. \end{aligned} \tag{21}$$

To cope with the fact that in many applications the size of the $R+1$ dimensions might differ, we propose the following procedure. Without loss of generality, let us consider the case in which $M_1 \geq M_2 \geq \ldots \geq M_{R+1}$. We start by estimating $\hat{d}$ with the modified EFT method considering the first unfolding only. If $\hat{d} < M_2$, we could have taken advantage of the second mode as well. Therefore, we compute the global eigenvalues $\lambda_i^{(\mathrm{G})}$ as in equation (20) for $1 \leq i \leq M_2$, thus discarding the $M_1 - M_2$ last eigenvalues of the first mode. We can obtain a new estimate $\hat{d}$. If $\hat{d} < M_3$ we could continue in the same fashion, by computing the global eigenvalues considering the first 3 modes. Clearly, the full potential of the proposed method can be achieved when all modes are used to compute the global eigenvalues. This happens when $\hat{d} < M_{R+1}$, so that $\lambda_i^{(\mathrm{G})}$ can be computed for $1 \leq i \leq M_{R+1}$.

Note that the R-dimensional extension described in this section can be applied to *any* model order selection scheme that is based on the profile of eigenvalues, i.e., also to the MDL and the AIC methods. The corresponding R-dimensional versions are obtained by replacing the eigenvalues of $\hat{\boldsymbol{R}}_{xx}$ by the global eigenvalues $\lambda_i^{(\mathrm{G})}$ defined in equation (20). Additionally, for computing the number of free parameters for the AIC and MDL methods and their R-D extensions, we propose to set the parameter *number of sensors* to the number of *global eigenvalues* and the parameter *number of snapshots* to N.

6. SIMULATION RESULTS

In this section we present simulation results demonstrating the performance of the proposed methods. Following the CFAR approach, the probability of false alarm is set to a constant for all signal to noise ratios. For simplicity, we set $P_{\text{fa}}(P) = 10^{-6}$ for

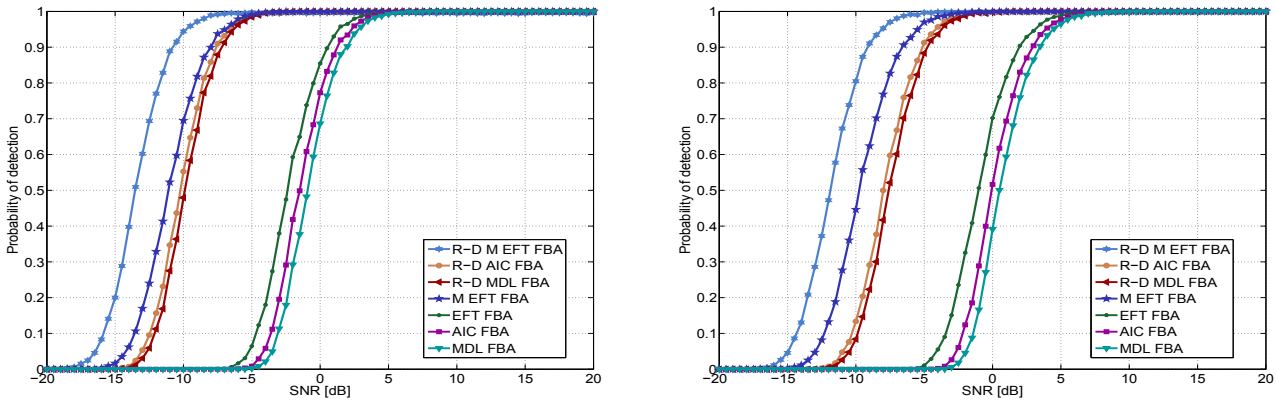

Fig. 4. Probability of detection vs. SNR considering a system with $N = 5$ snapshots, a 4-D array of size $M_1 = 5$, $M_2 = 5$, $M_3 = 5$, $M_4 = 5$. On the left-hand side, $d = 2$ sources are present, whereas on the right-hand side the same scenario with $d = 3$ sources is shown.

all values of P. It is therefore instructive to compare the probability of correct detection, i.e., $\Pr\left(\hat{d} = d\right)$ versus the SNR. We also assume that the noise samples are zero mean circularly symmetric complex Gaussian distributed and mutually independent with variance equal to σ_n^2. The spatial frequencies $\mu_i^{(r)}$ are drawn from a uniform distribution in $[-\pi, \pi]$. The damping factors $\zeta_i^{(r)}$ are set to 0. Consequently, forward-backward averaging is also incorporated. The source symbols are zero mean i.i.d. circularly symmetric complex Gaussian distributed with power equal to σ_s^2 for all the sources. The SNR at the receiver can then be defined as

$$\mathrm{SNR} = 10 \cdot \log_{10}\left(\frac{\sigma_{\mathrm{s}}^2}{\sigma_{\mathrm{n}}^2}\right). \tag{22}$$

Figure 3 depicts a scenario where $d = 3$ sources are impinging on a 3-D array of size $M_1 = 5$, $M_2 = 7$, and $M_3 = 9$, collecting $N = 10$ snapshots. We can clearly see that the R-D extension of the AIC, the MDL, and the EFT enhance the performance significantly. Also, the *modified EFT* (M EFT) described in Section 4 outperforms the original EFT of [4] and [8] by more than 7 dB.

Similarly, in Figure 4 we compare the proposed methods for a scenario where d sources are located in the far-field of a 4-D array of size $M_1 = 5$, $M_2 = 5$, $M_3 = 5$, and $M_4 = 5$. In this case, the number of snapshots N is set to 5. For the result shown on the left-hand side of Figure 4 d is set to 2. On the other hand, the right-hand side of Figure 4 depicts the same scenario with $d = 3$ sources. Again, the M EFT outperforms the EFT by more than 8 dB and the R-D extension provides a gain of more than 10 dB. Also, the R-D extensions of AIC and MDL improve the classical methods by more than 7 dB.

7. CONCLUSIONS

In this paper, we have presented enhanced model order estimation schemes for noise-corrupted multi-dimensional data sampled on an R-dimensional grid. Using the HOSVD of the measurement tensor, we obtain $R + 1$ sets of n-mode singular values of the measurement tensor that are combined to form *global eigenvalues*. Thereby, the accuracy of model order selection schemes that are based on the profile of the eigenvalues is improved significantly as compared to the matrix case. As an example, we have derived an R-D extension of the Exponential Fitting Test (EFT), which is particularly useful if only a small number of temporal snapshots is available. Moreover, we have shown how to extend classical model order selection techniques such as AIC and MDL to the R-D case. We have also described a *modified version of EFT* (M EFT) that improves the performance of EFT as originally published in [4] and [8]. Furthermore, we have shown how forward-backward averaging can be incorporated if the model order of a superposition of *undamped* R-D exponentials is estimated.

REFERENCES

[1] H. Akaike, "A new look at the statistical model identification", *IEEE Trans. on Automatic Control*, vol. AC-19, pp. 716–723, 1974.

[2] A. Barron, J. Rissanen, and B. Yu, "The minimum description length principle in coding and modeling", *IEEE Trans. on Information Theory*, vol. 44, pp. 2743–2760, 1998.

[3] L. de Lathauwer, B. de Moor, and J. Vanderwalle, "A multilinear singular value decomposition", *SIAM J. Matrix Anal. Appl.*, vol. 21(4), 2000.

[4] J. Grouffaud, P. Larzbal, and H. Clergeot, "Some properties of ordered eigenvalues of a wishart matrix: application in detection test and model order selection", in *Proceedings of the IEEE International Conference on Acoustics, Speech and Signal Processing (ICASSP'96)*, vol. 5, pp. 2463 – 2466, May 1996.

[5] M. Haardt and J. A. Nossek, "Simultaneous Schur decomposition of several non-symmetric matrices to achieve automatic pairing in multidimensional harmonic retrieval problems", *IEEE Trans. Signal Processing*, vol. 46, pp. 161–169, Jan. 1998.

[6] M. Haardt, R. S. Thomä, and A. Richter, "Multidimensional high-resolution parameter estimation with applications to channel sounding", in *High-Resolution and Robust Signal Processing*, pp. 255–338. Marcel Dekker, New York, NY, 2004, Chapter 5.

[7] A. Lee, "Centrohermitian and skew-centrohermitian matrices", *Linear algebra and its applications*, vol. 29, pp. 205–210, 1980.

[8] A. Quinlan, J.-P. Barbot, P. Larzabal, and M. Haardt, "Model order selection for short data: An exponential fitting test (EFT)", *EURASIP Journal on Applied Signal Processing*, 2007, Special Issue on Advances in Subspace-based Techniques for Signal Processing and Communications.

[9] F. Roemer, M. Haardt, and G. Del Galdo, "Higher order SVD based subspace estimation to improve multi-dimensional parameter estimation algorithms", in *Proc. 40th Asilomar Conf. on Signals, Systems, and Computers*, pp. 961–965, Nov. 2006.

[10] M. Wax and T. Kailath, "Detection of signals by information theoretic criteria", *IEEE Trans. on Acoustics, Speech, and Signal Processing*, vol. ASSP-33, pp. 387–392, 1985.

[11] G. Xu, R. H. Roy, and T. Kailath, "Detection of number of sources via exploitation of centro-symmetry property", *IEEE Trans. Signal Processing*, vol. 42, pp. 102–112, Jan. 1994.